Journal of Materials Chemistry A

ROYAL SOCIETY OF CHEMISTRY

PAPER

View Article Online
View Journal | View Issue

Cite this: J. Mater. Chem. A, 2022, 10, 21579

Production of energy-storage paper electrodes using a pilot-scale paper machine†

Patrik Isacsson, [ad] Karishma Jain, [b] Andreas Fall,[c] Valerie Chauve,[d] Alireza Hajian, ‡[b] Hjalmar Granberg,[c] Lucie Boiron,[d] Magnus Berggren,[af] Karl Håkansson, [c] Jesper Edberg, [e] Isak Engquist *[af] and Lars Wågberg *[bg]

Received 2nd June 2022
Accepted 20th September 2022

DOI: 10.1039/d2ta04431e

rsc.li/materials-a

The global efforts in electrifying our society drive the demand for low-cost and sustainable energy storage solutions. In the present work, a novel material concept was investigated to enable fabrication of several 10 meter-long rolls of supercapacitor paper electrodes on a pilot-scale paper machine. The material concept was based on cationized, cellulose-rich wood-derived fibres, conducting polymer PEDOT:PSS, and activated carbon filler particles. Cationic fibres saturated with anionic PEDOT:PSS provide a conducting scaffold hosting the activated carbon, which functions as the active charge-storage material. The response from further additives was systematically investigated for several critical paper properties. Cellulose nanofibrils were found to improve mechanical properties, while carbon black enhanced both the conductivity and the storage capacity of the activated carbon, reaching a specific capacitance of 67 F g^{-1}. This pilot trial shows that "classical" papermaking methods are fit for the purpose and provides valuable insights on how to further advance bio-based energy storage solutions for large-scale applications.

Introduction

The race towards replacing fossil fuels with renewable energy sources and eco-friendly large-scale energy storage systems is under an immense acceleration. This is in part due to a pull from societal and industrial actions and regulations as well as from a push generated by a rapid drop in the costs for energy harvesting technologies. However, as these renewable energy sources are intermittent, with the sun shining only in daytime and wind being highly irregular, balancing the power grids is becoming a challenge.[1] In order to solve this problem, any excess of produced energy should be stored for later use when demands are high. While many alternatives to such intermittent energy storage exist, the cost for electrochemical devices such as the lithium-ion battery (LIB) is expected to drop enough to become the technology of choice for most stationary applications by 2030.[2]

Although LIB technologies are considered as vital for energy storage in the shift in our energy systems, several inherent limitations such a high cost, short lifetime, poor safety characteristics and environmental hazards,[3] motivate the research for alternative energy storage technologies. Several alternative energy-storage technologies have emerged in the last decade, some of which based on bio-derived materials. They hold a promise for cheap and environmentally friendly energy storage.[4] A multitude of concepts have been developed to exploit lignocellulosic materials as key components in electrodes for energy storage, ranging from utilizing lignin as a redox-active cathode material in secondary batteries[5] to the use of the natural binding properties of cellulose as the key structural component in electrical double-layer capacitors (EDLCs).[6] These bio-based batteries and supercapacitors, sometimes referred to as paper batteries, have been designed and developed to provide environmentally friendly characteristics, both with respect to the material origins, production, operation, and their disposal/recycling specifications at the end of life.[7] Further, in contrast to traditional electrode fabrication methods, which are built around the approach of coating electrode slurries on metal current collectors,[8] paper electrodes also hold an inherent promise for higher production rates since paper-based technologies can be produced and converted into products at very large scales and fast line speeds.

[a]Laboratory of Organic Electronics, Department of Science and Technology, Linkoping University, 601 74 Norrkoping, Sweden. E-mail: isak.engquist@liu.se

[b]Department of Fiber and Polymer Technology, KTH Royal Institute of Technology, Teknikringen 56–58, SE-100 44 Stockholm, Sweden. E-mail: wagberg@kth.se

[c]RISE Research Institutes of Sweden, Bioeconomy and Health, Drottning Kristinas väg 61, SE-114 86 Stockholm, Sweden

[d]Ahlstrom-Munksjö Research Center, 38140 Apprieu, France

[e]RISE Research Institutes of Sweden, Digital Systems, Bio- and Organic Electronics, Bredgatan 35, Norrköping SE-602 21, Sweden

[f]Wallenberg Wood Science Center, Linköping University, Department of Science and Technology, Linkoping University, 601 74 Norrkoping, Sweden

[g]Wallenberg Wood Science Center, KTH Royal Institute of Technology, Teknikringen 56–58, SE-100 44 Stockholm, Sweden

† Electronic supplementary information (ESI) available. See https://doi.org/10.1039/d2ta04431e

‡ Present address: Department of Mechanical Engineering, Massachusetts Institute of Technology, 77 Massachusetts Avenue, Cambridge, MA 02139, USA.

To become industrially relevant, these new technologies need to first take the step from lab-scale production to pilot production protocols, which for the actual materials usually relates to up-scaling from the gram to kilogram scale. This critical step, unfortunately, jeopardies many promising technologies from finally reaching the market. One such example is graphene, which was first demonstrated in 2004 but just recently reached the market owing to the breakthroughs in scaling up manufacturing.[9] In this work, a similar step has been taken in paper electronics by the production of a bio-based "energy-storage paper" in a pilot-scale paper machine.

In the study of paper electrode systems, an often-used starting point is to employ nano-scaled cellulose fibrils, which makes it easier to exploit the molecular properties of cellulose and to create more well-defined systems.[10–14] For these materials, lab-scale preparation methods such as casting and oven drying are often selected. To study coarser systems with cellulose-rich macroscale pulp fibres, preparation methods with high material retention such as vacuum-assisted dewatering over filter papers[15,16] or stencil printing[17] are generally chosen as it facilitates material characterisation and analysis. Transferring these lab-prepared material concepts into papermaking conditions is not, however, a straightforward task. Using nanocellulose derivatives as the web-forming material alone is simply not possible due to its small fibre size and remarkable water retention properties.[18,19] Exchanging the nanoscale cellulose fibrils into macroscale pulp fibres would make a such transition easier, but the forming section in papermaking, where the fibre suspension is drained through a coarse wire, puts further demands on a well-designed system. As the fibres themselves are insulating and mainly have the role of a hosting scaffold for the electroactive filler materials, the system needs to combine a high retention of these active components in the web with fast dewatering rates to achieve a satisfying performance along with good processability.

Furthermore, an electronically conductive network is required for efficient transfer of electrons to the sites of charge storage. *In situ* polymerization of conducting polymers such as polypyrrole on pulp fibres has been proposed and demonstrated in large scale, although the performance has not been disclosed.[20] The toxicity of the monomers for many common conducting polymers introduces yet another query, since wastewater treatment plants for pulp- and papermaking normally are adapted for handling fibre fragments and mineral fillers rather than toxic pollutants.

An alternative approach is to use ready-made conducting polymer systems as a conductive additive, not at least since the combination of conducting polymers and carbon materials can form well-performing electrode materials for supercapacitors.[21] Recently, Belaineh and co-workers[22] demonstrated poly(3,4-ethylenedioxy-thiophene) polystyrene sulfonate (PEDOT:PSS) to work excellently in combination with activated carbon (AC), showing that not more than 10 wt% PEDOT:PSS is needed for creating efficient electronic links between the capacitive AC particles. Compared to AC and cellulose-rich fibres, PEDOT:PSS is the most cost-critical component in the material concept, which stresses the need for good retention of the PEDOT:PSS.

Previous attempts of adding anionic PEDOT:PSS to a papermaking process has been hindered by the inability of the nanosized particles to adhere to anionic cellulose fibres or fibrils in the dispersion. This has been shown in previous studies where the preparation of cellulose-based electrodes explored the use of anionically charged cellulose or bacterial cellulose.[23] Due to the anionic nature of most conducting materials, the material loading on cellulose is low resulting in difficulties to retain these materials in a paper making process.[24] To retain the polymers in the sheet, it is necessary to utilize different retention strategies which often results in aggregation of the conducting polymers. This usually decreases the efficiency of the polymer to create the necessary conducting network.

To avoid these problems, cellulose can be modified to increase the interaction between conducting materials and cellulose without sacrificing the excellent conductive properties of the PEDOT:PSS. This work investigates the use of cellulose-rich wood-based fibres functionalized with cationic quaternary trimethylammonium groups (Fig. 1A). The present method solves the previous issues with adhesion of the conductive polymer to the fibre network and enables an even deposition of the polymer onto the fibres in combination with the necessary fast dewatering rates for up-scaled production. The addition of fixed positively charged groups along the fibres enables homogenous electrostatic adsorption of negatively charged PEDOT:PSS nanoparticles, which creates a percolating conducting network for the active materials (Fig. 1B).

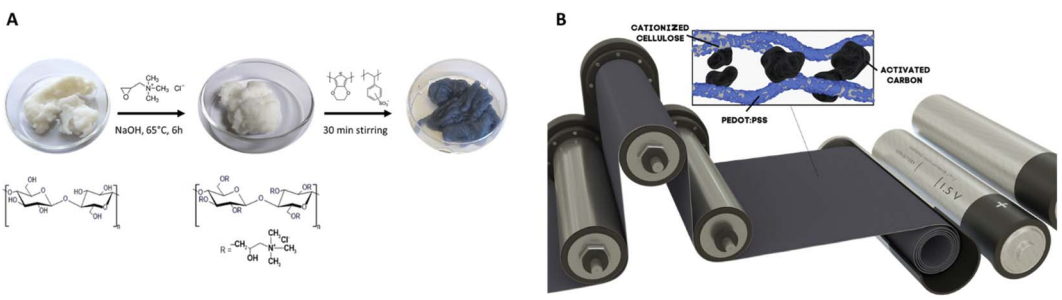

Fig. 1 The main material concept studied in this work. The selected papermaking chemistry for the paper machine trials with the cationization of cellulose-rich pulp fibers with glycidyl trimethylammonium chloride and subsequent PEDOT:PSS adsorption (A) and a schematic description of the material concept and the selected process (B).

In this work, AC was selected as the main active, charge storing material. Furthermore, the addition of carboxymethylated cellulose nanofibrils (CNF) and/or conductive carbon black dispersed by CNF (CB:CNF)[25] were used to enhance the mechanical properties of the prepared paper and to improve the conducting properties of the fibre-based system. The effects were evaluated statistically for material properties such as mechanical strength, conductivity, and electrochemical charge storage performance. Finally, the optimal material combinations were used to assemble a full supercapacitor device. To our knowledge, this is the first study where cationically charged cellulose-rich fibres are used for large scale production of paper electrodes for energy storage applications.

Results & discussion

This work is divided into different parts. First, pre-trial studies are reported, in which the material formulations were evaluated in lab scale evaluations. Next, the processability of the material concept in the pilot paper machine is in focus. Here, in-process measurements are combined with structural characterisations of the formed papers to understand factors impacting the processing of the papers. Further, the effects of the additives CNF and/or CB:CNF on mechanical and electrochemical properties are reviewed and discussed. Since papers constitute a heterogenous material system, a statistical approach using two-way analysis of variance (ANOVA) was applied to sort out effects from the different additives. Finally, an EDLC device has been assembled and characterised.

Pre-trial laboratory evaluation of the material concept

The reaction is the nucleophillic addition of epoxy groups in glycidyl trimethylammonium chloride to the surface hydroxyl groups of cellulose. To establish the surface modification, the FTIR peak at 1480 cm^{-1} which is representative of methyl groups in trimethyl ammonium was used previously.[26,27] The FTIR spectra of the unmodified and cationic fibers used in this work is shown in (Fig. S1A†). The zoom-in spectra between 1300 and 1600 cm^{-1} shows a peak at 1480 cm^{-1} (Fig. S1B†), which is absent in the unmodified pulp. Therefore, showing the presence of trimetheylammonium groups on cationic fibers.

To understand the retention of the AC, retention trials were performed with cationic polyacrylamide (C-PAM) as the retention aid. The cationic fibres were pre-treated with PEDOT:PSS in order to avoid aggregation of this active component, which otherwise would have led to a concomitant loss in conducting efficiency. The addition of 0.2 wt% C-PAM increased the total retention to more than 90% (Fig. S2†). Hence, this retention aid was selected for the papermaking process.

Laboratory-prepared hand sheets were made from the combination of cationic pulp fibres, PEDOT:PSS and AC and were then used for electrochemical characterisation. As shown in Fig. S3,† AC-loaded papers with PEDOT:PSS pre-treated cationic fibres showed a halved internal resistance and a 17 times increase in the areal capacitance as compared to non PEDOT:PSS cationic fibres. As the capacitance of sheets with PEDOT:PSS alone is negligible (Fig. S3†), the main role of the PEDOT:PSS may be in its contribution of electrical conductivity. The conductivity along the fibres in turn helps creating a percolating network, which can be decisive for exploiting the capacitive property of the loaded AC. This is in line with previously reported work,[22] where it was found that < 10 wt% cellulose fibres rather than directly increasing the capacitance PEDOT:PSS is needed to reach an optimum specific capacitance in the resulting system where AC makes up the rest of the electroactive material. This could be compared with the present work, where PEDOT:PSS constitutes of less than 1% of the total paper weight, *i.e.* the use of cationized fibres allows for an efficient utilization of the PEDOT:PSS properties.

Production of electrode paper rolls on a pilot paper machine

A 2 × 2 experimental matrix was constructed in order to test the effects of adding CNF and/or CB:CNF to the formulations (Table 1). CNF was expected to contribute with improved mechanical properties of the paper, and the CB:CNF was hypothesized to contribute with an increased electric conductivity in addition to that of PEDOT:PSS.

All the four formulations exhibit good rentability on the pilot paper machine, where the wet strength of the papers is enough to enable the passing from the forming section to the pressing section. Photos of the paper line along the pilot machine (Fig. S4†) show a good marginal for the water line to the end of the forming section, and a successful winding of a roll after the drying sections. All the resulting papers have a grammage around 100 g m^{-2}, with an achieved thickness varying from 223 to 265 μm (Fig. S5†). One roll of about 10 meters in length were produced from each formulation.

As the white water (*i.e.* paper making filtrate) was black, it was clear that the retention is not perfect but enough to allow for a decent rentability on the pilot paper machine. As the performance of the composite as an EDLC electrode clearly

Table 1 Experimental matrix for the pilot trial. Dry wt% ratios given for the four formulations (*i*)–(*iv*) with the components cationic pulp with PEDOT:PSS (CP:PP), activated carbon (AC), carboxymethylated cellulose nanofibrils (CNF) and carbon black dispersed by CNF (CB:CNF). All formulations also included 0.2 wt% C-PAM as a retention aid

	Without CNF		With CNF	
Without CB:CNF	*i*		*ii*	
	CP:PP	AC	CP:PP	AC
	51.2%	48.6%	48.9%	48.6%
	CNF	CB:CNF	CNF	CB:CNF
	—	—	2.3%	—
With CB:CNF	*iii*		*iv*	
	CP:PP	AC	CP:PP	AC
	53.2%	45.9%	52.2%	44.6%
	CNF	CB:CNF	CNF	CB:CNF
	—	0.7%	2.3%	0.7%

benefits from having a high loading of the active material, a poor retention should naturally be avoided.

Thermogravimetric analysis (TGA) was conducted to determine the composition of the web. The thermal decomposition patterns of the main components AC and pulp, which points of inflections were used as material-specific markers, were compared with those of the formed papers (Fig. S6†). The inflection points of pulp (350 °C and 500 °C) corresponded well to previously reported thermal degradation patterns[28] as well as the inflection points in the formed paper. In line with other reported TGA of AC composites,[29] the thermal stability of AC (inflection point 725 °C) was considerably reduced when being included in the papers (around 600–650 °C).

The results of the TGA revealed a clear difference between samples with and without CNF, where adding CNF to the formulation resulted in a decreased loading of carbonized materials (Fig. S7†). This points out a poorer retention of the AC in the CNF formulations, probably due to a non-ideal balance of the charges in the system as the CNF-formulation was added. The samples with CNF also display a higher formation number (Fig. S8†), which reflects a poorly distributed fibre network and an aggregated structure of the fibres in the paper.

This is somewhat surprising as there commonly exists a trade-off between good formation and filler retention, although these types of multicomponent system have a more complex relation between retention and formation.[30] An explanation to this deviation could be found in the charge balance of the system. While the pH in all formulations was stable at pH8, the cationic demand was clearly higher for formulations including CNF (Fig. S8†). This difference is most probably related to the high anionic charge density of CNF which is not compensated by the amount of C-PAM added to the formulations. The balance between the C-PAM and the negative charge of the AC, measured as a ζ-potential of −30 mV using DLS-measurements, is hence disturbed by the addition of the negative CNF which in turn leads to a decreased retention of the AC in the paper. In future studies this negative impact can be balanced by a change in the order of addition of the components as well as their relative amounts.

Scanning electron microscopy (SEM) images of the paper surfaces show how this affects the morphology of the papers (Fig. 2A–H). The papers with CNF show a more aggregated structure of the carbon particles compared to those without CNF. Inadequate dosage of retention aids, increased flocculation and more aggregated filler particles is known to lead to a one-sided filler distribution.[31,32] This uneven *z*-distribution of fillers is also observable in the paper profiles when SEM/EDX analysis was performed on paper cross-sections. On the obtained elemental materials maps (Fig. 2I–L), it was expected to observe sulphur and nitrogen from PEDOT:PSS and the cationic groups in the pulp fibres, but the low concentrations of the elements was below detection limit. On the other hand, oxygen (representative of the fibres) and carbon (mainly from the AC) were easily detected which gave a clear view of the filler distributions in the papers. The sample with CNF but without CB:CNF(ii) indeed stood out with a skewed concentration profile of AC throughout the *Z*-direction of the paper (Fig. 2J), showing that the filtration retention mechanism dominates in that system.

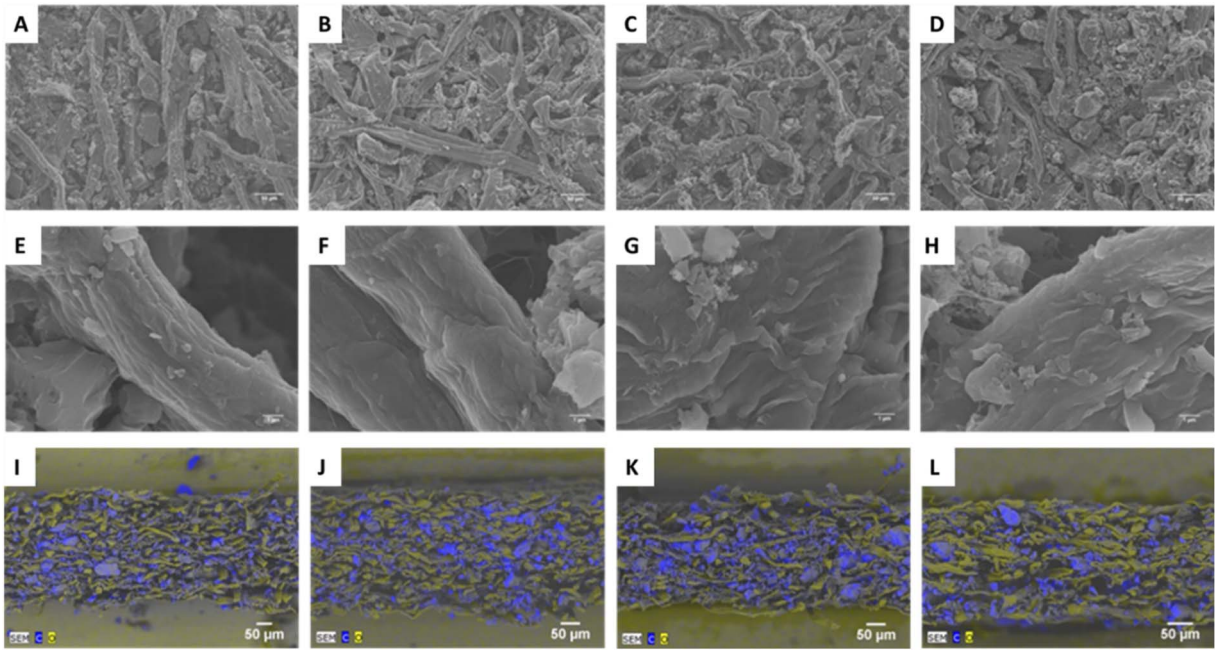

Fig. 2 Scanning electron microscopy images of the paper electrodes. SEM images of papers (top), zoom-in images of fiber surface (middle) and cross-section SEM/EDX images (bottom) of the papers made from formulations (i) (A, E and I), (ii) (B, F and J), (iii) (C, G and K) and (iv) (D, H and L). On the EDX maps, the oxygen-rich cellulose fibers appear yellow while the carbon-rich AC and CB filler particles appear blue. More aggregated structures can be observed for formulations (ii) and (iv), and a skewed filler distribution profile can be observed for formulation (ii) in the cross-section (J).

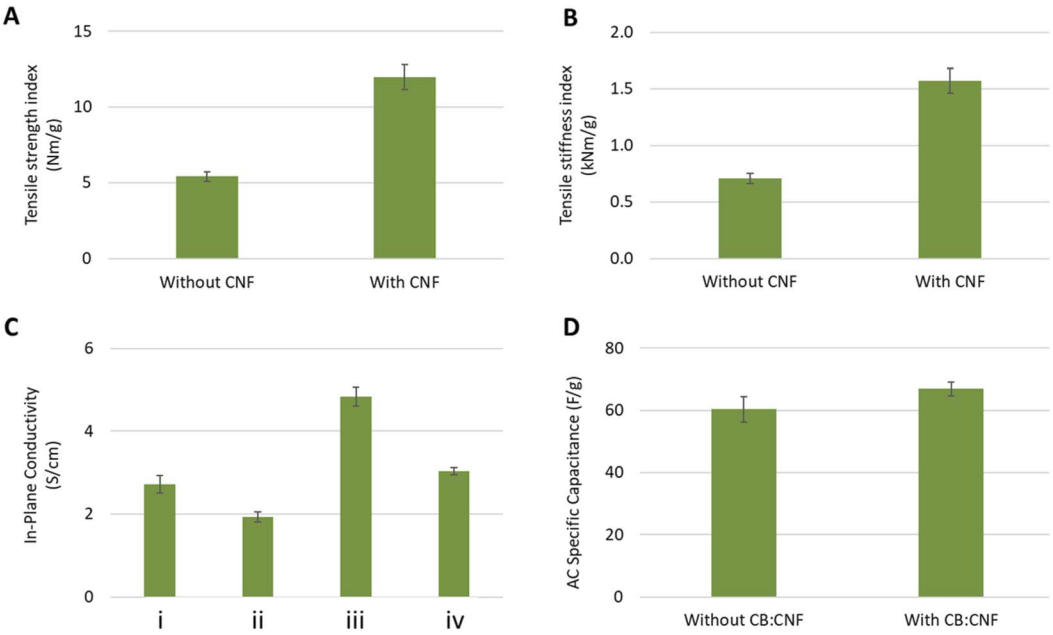

Fig. 3 Effects of different additives on the paper electrode properties. The mechanical properties evaluated as the tensile strength index (A) and the tensile stiffness index (B) are clearly affected by adding CNF, which is also the case for the in-plane conductivity (C). Adding CB:CNF has also an effect on the conductivity (C), along with a small but significant effect on the specific capacitance per mass unit AC (D). Error bars represent 95% confidence intervals.

Mechanical properties

All tested mechanical properties display a significant effect from CNF ($n = 20$; $p < 0.00$). Both the tensile strength index as well as the tensile stiffness index in the papers with CNF is more than twice of those without (Fig. 3A and B). These papers reached an average tensile strength index of 12.0 Nm g^{-1} and an average tensile stiffness index of 1.6 kNm g^{-1}. It is not consistent with the formation values of the same papers, as papers with poorer formation usually display lower strength.[33] This should support the assumption that CNF is useful as a dry-strength agent, which is in line with previous reports of adding cellulose nanofibrils to paper formulations.[34] The lower loading of AC in the CNF-containing papers should, however, also result in better mechanical properties due to the inverse relationship between filler content and both tensile strength and tensile stiffness.[35] In general, the mechanical properties of the highly filled AC papers are low and need to be improved in the future investigations. This is important both for the handling of the papers in the process and for the development of an efficient percolating network which is so important for the conductive properties of the prepared material.

Electrical and electrochemical properties

The in-plane conductivity of all the formed papers was in the magnitude of about 1–10 S m^{-1}, although significant differences were detected between the papers ($n = 9$, $p < 0.00$ for all combinations). Adding CNF has a negative effect on the conductivity, while the addition of CB:CNF increases the conductivity (Fig. 3C). A similar difference would have been expected to be observed also for the internal resistance in the 3-electrode measurements, as the internal resistance of an electrode partly depends on its electrical conductivity. However, no differences were possible to distinguish (Fig. S9†). The large sample standard deviations of 12–26 Ω, which can be compared with the average internal resistance of 41 Ω, do not allow a comparison between the different papers. It can therefore not be concluded if the addition of CNF and/or CB:CNF affects the internal resistance. Overall, an internal resistance of 41 Ω is a high value compared to other works on EDLC supercapacitor electrodes,[36,37] which explains why the discharge current level had to be set to as low as 0.2 A g^{-1} AC in order to have reliable measurements (Fig. S10†). It's not understood what is causing this high internal resistance, nor the large sample standard deviation, why it is important to investigate the sources of internal resistance in the continued research on this material concept.

The measured specific capacitance per mass unit paper ranged from 23.6 to 29.4 F g^{-1}, where the papers with less loading of AC displayed a lower capacitance. Normalizing the specific capacitance to the loading of AC (*i.e.* normalized to the capacitive material mass), a small but significant difference ($n = 10$, $p = 0.02$) can be observed between the papers with CB:CNF and those without (Fig. 3D). The average AC specific capacitance without CB:CNF is 60 F g^{-1} and 67 F g^{-1} with CB:CNF. This implies that adding CNF to the formulation does not hamper the electrochemical performance, while adding CB:CNF results in an increased accessible charge storage area.

It can appear contradictory that CNF cause a lower electrical conductivity but no decrease in AC specific capacitance, while the addition of CB:CNF increase both the electrical conductivity and the AC specific capacitance. Nanofibrillated celluloses such

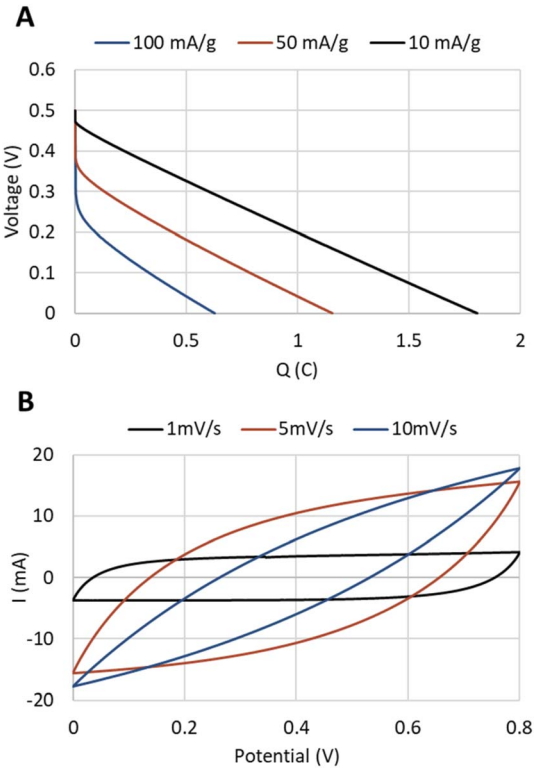

Fig. 4 Characteristics of the EDLC device. (A) Discharge at different discharge currents and (B) cyclic voltammetry at different scan rates.

as CNF is known to form insulating barriers between the conductive particles,[14] and although no such phenomena can be observed in the SEM images, it can still be assumed that CNF limit the available contact area between the conducting PEDOT:PSS-covered fibres and thus give a decreased conductivity. However, it does not necessarily affect the capacitance, as the achieved capacitance is a measure of the amount accessed AC particles. Therefore, it can be anticipated that adding CNF reduces the number of electrical contact points, but not reduce the number of accessed AC particles. CB:CNF, on the other hand, enables a supply of small-sized conductors in addition to the conducting fibers, which increase the electrical contact points between the fibres and forms a more efficient percolating network.[38] They have also the ability to provide a finer branching network of conductors, which enables a higher probability of contacting AC particles out of reach for the coarser conducting fibers. This corresponds well both with the observed increased conductivity as well as the increased AC specific capacitance seen for papers with CB:CNF added.

Electrochemical impedance spectroscopy (EIS) analysis on paper samples were performed using the same equipment, cell setup and sample preparation method as for the other electrochemical measurands. Fig. S6 in ESI† shows the acquired spectra, presented both as Bode plots and as Nyquist plots. The shape of each graphs gives valuable qualitative information. However, modeling is usually required to get a more detailed picture of the various charge transport and storage phenomenon dominating the impedance at different frequencies. Equivalent circuit modeling (ECM) is one of the simplest ways of modeling EIS data, and it has been widely used to study various electrochemical devices. One such system is that of porous electrodes, which are often modelled using a transmission with pore size distribution (TLM-PSD)[53]. Yoo *et al.*[54] used the TLM-PSD to model electrodes containing activated carbon particles used for supercapacitor applications. [1] In their work, the system was described as having three main components related to (1) the bulk electrolyte, (2) the electrolyte–electrode interface, and (3) the porous bulk of the electrode.

In our work, we have used a similar approach to derive the ECM shown in Fig. S11A.† Here, R_E is the bulk electrolyte resistance, R_I, CPE_I and Z_W is the resistance, capacitance and diffusion elements of the interface between electrolyte and electrode, and R_B and CPE_B is the inter- and intra-pore resistance and capacitance in the bulk of the electrode. Constant phase elements (CPEs) where used instead of capacitors to account for the distributions if pore seizes as well as the rough surface of the interface. In addition to these elements, an inductor (L) was added to account for the high-frequency behavior. Such inductive behavior could be caused by the cables and the cell in the measurement setup. As can be seen in Fig. S11,† the model could be used to accurately fit the measurement data for all samples. The bulk resistor and the interfacial elements comprises the Randles circuit, which is often used to describe planar electrodes.

However, these elements alone were not enough to reproduce the capacitance of the samples, as measured using chronoamperometric methods. By adding the bulk elements, the fitting became more accurate, and we got two sets of capacitance values: one in the range of 100 μF cm^{-2} (CPEI) and one in the range of 100 mF cm^{-2} (CPEB). This corresponds well with the expected values of a flat surface electric double layer (usually 10–100 μF cm^{-2}) and the capacitance values measured for the sample during charge–discharge measurements (100–300 mF cm^{-2}). This model can be used in future studies to give new insights into the charge storage properties of paper supercapacitors.

The cycling stability of the papers was qualitatively investigated by cycling samples from paper iii and iv at a 1A g^{-1} discharge rate for 5′000 cycles (Fig. S12†). Both papers demonstrated a similar pattern, where the capacitance increased over the first 500 cycles, which has also been reported elsewhere.[39] After the initial decrease, the capacitance dropped to around 87% after 5 000 cycles which is in line with several well-performing EDLC supercapacitor electrode materials.[40,41]

The internal resistance had a mirrored development, with a decrease until 500 cycles and then an increase. Interestingly, both papers demonstrated peaks in the internal resistance around 1′500 cycles which do not have any counterpart in the capacitance. As only 1 sample per paper was evaluated, the results cannot tell if there's a difference between a paper without added CNF (*iii*) or with (*iv*). Further, as the stability and performance of electrode materials are dependent on the conditions in assembled devices[42] where not at least the electrolyte plays an important role,[43] a more in-depth analysis of the

electrode stability would require a more structured analysis of the material in different relevant electrolytes.

To demonstrate the applicability of these papers as supercapacitor electrodes, an EDLC device was constructed with circular paper electrodes having a diameter of 5.5 cm (Fig. S9†). As an aqueous KCl electrolyte is not preferable in the device setting given the limited potential range and corrosion on the aluminum current collector used, an ionic liquid was used to enable a comparison with half-cell measurements. The paper based EDLC displayed a linear discharge characteristic for a supercapacitor, although the specific capacitance was clearly affected by the discharge current (Fig. 4A). For example, a discharge current at 100 mA g^{-1} AC resulted in an AC specific capacitance of 40.2 F g^{-1} while a discharge current of 10 mA g^{-1} AC reached 72.5 F g^{-1} AC. This further points out the need for lowering the internal resistance in future trials, but the EDLC device also demonstrates that the material can be used as in the targeted application, as a paper electrode in a supercapacitor.

Conclusions

Electrode papers for an energy storage application can be produced on a pilot-scale paper machine, with up to 99% of bio-based and 100% organic materials used in the formulations. Pre-trial laboratory hand sheet studies demonstrate that a combination of cationised cellulose-rich wood based fibres with very small amounts of electrostatically adsorbed PEDOT:PSS can create a conducting percolating network to connect the charge-storing AC particles.

This material concept can successfully be transferred to paper-making conditions on a pilot scale. Adding CNF to the formulations lower the retention of the AC, thus resulting in a lower capacitance per area. The poorer retention is likely caused by insufficient charge balancing in the systems when adding highly anionic CNF to formulations without a detailed adjustment of the dosage of the cationic retention agent. On the other hand, it is suggested that the CNF is important for improving the mechanical properties, although the contribution from CNF is not possible to exactly quantify since the produced papers with CNF also had lower filler contents.

Despite having a considerably higher amount of binders in this work compared to commercial, coated supercapacitor electrodes,[44] the achieved AC specific capacitance of 67 F g^{-1} can be compared with the 100 F g^{-1} that commercial supercapacitor electrodes has reached after decades of developments.[45] Still, the capacitance could be even higher. In other works which have used similar grades of AC from the same supplier as references, the AC reaches specific capacitances of 160–180 F g^{-1}.[46,47] Exploiting the full capacitance of the AC should therefore be an attractive route for enhancing the electrode specific capacitance, in contrast to increasing the AC filler content which should have a substantial negative effect on the mechanical properties.

Since both the in-plane conductivity and the AC specific capacitance is positively affected by adding conducting CB:CNF, it could be viewed as plausible that further improvements of the conducting percolating network should indeed result in an increased charge-storage performance. Further, as CNF does not impair with the AC specific capacitance, this additive should be a good alternative to enhance mechanical properties without limiting the electrochemical performance.

Nevertheless, the formed paper electrodes can store significant amounts of charge without having been optimized, and the higher share of binders does also bring benefits. As the cellulose fibres themselves swells in the electrolyte and provides a channelling network for the electrolyte in the electrode bulk, these paper electrodes have the potential to enable thick electrodes with preserved AC-electrolyte contact. The present paper electrodes have a grammage around 100 g m^{-2} but could theoretically be made several times thicker.

The additions of CB and CNF have significant effects on the in-plane conductivity of the papers, where an increase in conductivity was observed when adding CB while the addition of CNF decreased conductivity, probably due to a poorer retention. However, the specific capacitance per mass unit of AC was not affected by the addition of CNF, while it did show a significant increase from 60 to 67 F g^{-1} when adding CB:CNF.

This points out two important learnings; (1) CNF can be used as an additive to enhance mechanical properties without impairing with electrochemical performance and (2) further improvements of the conducting percolating network are probably necessary for accessing a larger charge storage site area of the AC.

The decent electrode properties in general combined with the good runability, demonstrates the feasibility of using paper making techniques for fabricating supercapacitor electrodes. Further, this work expands the knowledge about critical aspects in the design of the formulations and process design, and advances the technological frontier of paper-based energy storage solutions.

Experimental

The materials

Preparation of cationic pulp. To prepare cationic cellulose fibres, quaternary trimethylammonium groups are grafted on cellulose (Fig. 1). The reaction was performed according to the procedure by Pei *et al.*[48] with some modifications. Briefly, 400 g (dry weight) of a softwood sulfite dissolving pulp (Domsjö Dissolving plus, Domsjö Fabriker AB, Sweden) was mixed with 4.78 M NaOH (Sodium Hydroxide pellets, VWR) and left for 10 min. Afterwards, 612 g of isopropanol and 400 g of glycidyl trimethylammonium chloride (GTMAC, 99.9% purity, Sigma Aldrich) were added and the reaction mixture was mixed thoroughly.

The reaction was carried out at 65 °C for 6 hours in a hot water bath. The plastic bag with the reaction mixture was taken out every 1 h to knead the bag to mix the pulp for homogeneous reaction. The reaction mixture was neutralized with hydrochloric acid, filtered and washed thoroughly with deionized water. In total 2 kg of the cationic pulp was prepared for the pilot paper machine trials. The obtained charge density of pulp, measured with polyelectrolyte titration, was 250 ± 50 μeq g^{-1}.

Adsorption of PEDOT:PSS to pulp. PEDOT:PSS saturated fibres were prepared according to the following procedure (Fig. 1B). A fibre dispersion at 2 g L^{-1} was mixed with PEDOT:PSS (10 g L^{-1}, Orgacon ICP 1050, Agfa) dispersion and stirred for 30 min. The fibres were then filtered and washed thoroughly with deionized water to remove unadsorbed PEDOT:PSS. The adsorbed amount of PEDOT:PSS was calculated based on concentration of PEDOT:PSS left in the solution after saturation. The amount adsorbed was 0.75–1.5 wt% PEDOT:PSS depending on the added amounts.

Preparation of CNF and CB:CNF. The carboxymethylated cellulose nanofibrils (CNF) was produced from a softwood sulphite dissolving pulp (Domsjö Dissolving plus) from Domsjö Fabriker AB, Sweden. The pulp was carboxymethylated to a degree of substitution (DS) of 0.1, according to Wågberg *et al.*[49]

After the carboxymethylation, the pulp was homogenized (Microfluidizer M-110 EH, Microfluidics Corp., USA) one time at 1700 bar at 2 wt%, using two chambers with smallest dimension 200 μm and 100 μm, respectively, in series.

Carbon black (CB) was acquired from Fisher Scientific with the brand name: Thermo Scientific Alfa Aesar 039724.A1. The CB:CNF (10 : 1) mixture was prepared by adding 250 g CB to 1250 g CNF at 2 wt% and 4.75 g deionized water, where after the mixture was passed through the above-mentioned homogenizer at 400 bar and two serial chambers with smallest dimension of 400 μm and 200 μm, respectively.

Preparation of ionic liquid. 1-Ethyl-3-methylimidazolium ethyl sulfate (EMIM-Es) hydroxy ethyl cellulose (HEC), bought from Sigma Aldrich, were mixed in a ratio of 19 : 1 and heated to 110 °C on a hotplate until becoming a uniform gel, after which the mixture was allowed to be cooled and stored in room temperature before use.

Materials used as received. Activated carbon (AC) made from steam activated wood charcoal (Norit® A Supra, Acros Organics) was selected as the main charge storage material. Cationic polyacrylamide (C-PAM) was selected as retention aid. For the lab trials, Eka PL 1510 CPAM was used, and a corresponding C-PAM (Kemira Fennopol K4230 T) was used in the pilot trials.

Paper fabrication

Retention laboratory trials. Retention trials were performed using a Britt Dynamic Drainage Jar and a standard screen with pore size of 76 μm (125 P). The pulp was diluted to 5 g L^{-1} by mixing at 1000 rpm and a volume of 500 ml was used. The additional components were added sequentially with 30 s interval in the order of AC, CB:CNF and lastly C-PAM 1510. A 100 ml sample was taken after an additional 30 s and the concentration was determined and compared with the added material to result in a retention value.

Hand sheets preparation. To test the effect from PEDOT:PSS on the performance of the system before moving to pilot scale, laboratory hand sheets were prepared using a Rapid Köthen sheet former, PTI Pettenbach, Austria, with automatic couching and drying. Three hand sheets were prepared; cationic pulp with PEDOT:PSS only, cationic pulp without PEDOT:PSS but with AC and thirdly all materials combined. The laboratory hand sheets were evaluated electrochemically as described below.

Pilot paper trial. The pilot trial was designed as a factorial experiment, where a matrix of four different formulations was used to determine the effects of added CNF and/or CB (Table 1). All four formulations were based on AC and PEDOT:PSS-adsorbed cationic pulp, why the first formulation consisted only of these components to act as a reference. The second formulation was chosen to include CNF, a third one including CB:CNF and the fourth contained both CNF and CB:CNF. All formulations included 0.2 wt% C-PAM as a retention agent.

The pilot production of the electrode papers was carried out on a pilot-scaled, 20cm-wide fully equipped paper machine at Ahlstrom-Munksjö's R&D center located in Apprieu, France. The different wet-end formulations were prepared in chests before being pumped into the headbox at a consistency in the range of 6–6.7 g per liter. The web speed was set to 1 meter per minute, a speed which allows orientation of the fibres while allowing manual handling of the paper along the machine. Edges were trimmed in the forming section using waterjet cutting. The web was manually passed from the forming section to the two pressing nips (each set to 2 kg) and subsequent drying sections. The first drying section held a temperature between 138–180 °C and the second drying section between 124–155 °C. The formed paper, with a moisture content of about 6%, was collected as 10 meter-long webs winded on rolls. The cationic demand was measured on samples from the white-water using a Mütek PCD03.

Material characterisation

Thermogravimetric analysis. Differential thermo-gravimetric analysis (TGA) was performed using a Mettler Toledo DSC1 in ambient atmosphere and 20 °C min^{-1} heating rate. Reference measurements on the PEDOT:PSS-adsorbed cationic pulp, AC and CB:CNF were used to calculate the different components in the formed papers, by exploiting the different thermal degradation patterns of cellulose and carbonized materials.[50]

Scanning electron microscopy. Hitachi S-4800 Field-Emission Scanning Electron Microscope (FE-SEM) was used for studying paper rolls surfaces. All the samples were coated with Pt/Pd to avoid charging in SEM. Cross-section samples of the paper cut perpendicular to the machine direction were prepared using a Leica histological microtome. Cross-sections were imaged using a scanning electron microscope (SEM) (Zeiss, EVO50 LaB6Tip) and an energy-dispersive X-ray spectroscopy (EDX) (Bruker, Quantax 200 SDD 30 mm^2). On the obtained X-ray maps, oxygen was used as a marker for the pulp fibres, and carbon was used as a marker for the activated carbon.

Mechanical testing and formation. The mechanical properties were determined in the machine direction (MD) according to ISO1924-3 and the thickness according to SCAN-P 88:01 with 10 measurements performed per paper. The formation was determined by the β-radiography method.[51]

Dynamic light scattering (DLS). Zeta potential measurements were performed using DLS with backscattering detector (Zetasizer ZEN3600, Malvern Instruments Ltd U.K.).

Fourier-transform infrared spectroscopy (FTIR). FTIR of unmodified and cationized fibers was performed using PerkinElmer Spectrum 100 FTIR equipped with a diamond ATR (attenuated total reflection) crystal (Gaseby Specac Ltd, UK). The spectra was recorded at room temperature and averaged over 16 scans with a 4 cm^{-1} resolution.

Conductivity. Electrical sheet resistance was measured using a four-point probe system (Ossilla). For the hand sheets, each sample was probed and measured at three different points close to the center of the sample. For the machine-produced papers, a 6 cm wide cross strip of each paper was collected on which three probing positions was used; left edge, center and right edge in order to investigate any cross-direction effect on the conductivity. For each position, three measurement points were used.

The sample thickness was measured using a micrometer caliper. An average thickness, taken from three different points, was used together with the sheet resistance measurements to calculate the sample in-plane conductivity.

Electrochemical characterisation. 5 quadratic 1 cm patches were prepared with a laser cutter (Trotec Speedy 300) for each sample for electrochemical characterisation. Wet-proofed (polytetrafluoroethylene-impregnated) polyacrylonitrile carbon fibre sheets (Toray carbon paper) were chosen as a conducting support for the patches. The carbon paper was taped on one side with polyimide (Kapton) tape for improved mechanical stability, after which 1.5 cm wide supports were prepared from the taped sheets. The sample patches were mounted on individual supports by gluing them on the tape-free side using a carbon ink (7102 Carbon Conductor, DuPont), cured on a hot plate (150 °C) for 10 minutes.

The electrochemical characterisations were performed with a 3-electrode setup in a cell containing 20 ml 1 M KCl_{aq}, with a 2 × 2 cm activated carbon felt as counter electrode and an Ag/AgCl reference electrode. A potentiostat (Ivium Octostat5000) was used along with Ivium potentiostat software. For each characterisation, the open circuit potential (OCP) *vs.* Ag/AgCl was used as the starting point for the measurements.

Galvanostatic charge/discharge measurements were carried out with a set of current levels for one of the samples, after which every sample were investigated at current of 0.9 mA (approximately 0.2 A g^{-1} AC), with a voltage maximum of OCP + 0.5 V. Cyclic voltammetry was done in the potential window of OCP ±0.5 V at a scan rate of 10 mV s^{-1}.

Device assembly and characterisation. Circular paper electrodes (⌀ = 5.5 cm) from formulation (iii) as well as circular separators from cleanroom wipes (⌀ = 6.0 cm) were prepared with a laser cutter (Trotec Speedy 300). The laser-cut patches were mounted on the carbon-printed collectors prepared in previous work (Say *et al.* 2020) by gluing them using a commercial carbon ink (7102 Carbon Conductor, DuPont), which then was cured on a hot plate (100 °C) for 30 minutes.

A ring of double-sided tape was mounted around the glued papers on both collectors. The papers were soaked with the ionic electrolyte and left on a hotplate at 100 °C. After 1 hour's soaking, a cleanroom wipe was mounted on top of one of the papers, partially overlapping the tape. The structure was then laminated and sealed by mounting the separator-free side on top of the separator and the double-sided tape (Fig. S9†). The assembled device was electrochemically characterised using an Ivium Octostat5000 potentiostat along with Ivium potentiostat software. Cyclic voltammetry was done in the potential window of OCP ±0.5 V at 10 mV s^{-1} scan rate.

Statistical analysis. Two-way analysis of variance (ANOVA) with repeated measures was performed in order to explore effects of CNF and/or CB:CNF additions in the paper pilot trial. The analysis was performed assuming a normal distribution of the data and a significance level of $\alpha = 0.05$ was set to determine if the null hypothesis should be rejected.

In order to give a clearer visualization of the trends in the long-cycling experiments, the data were processed with the exponentially weighted moving average (EWMA) technique.[52] Here, the processed value z_i is a combined value of the value x_i and the precedent calculated value z_{i-1}. The weight of the value x_i is given by the constant λ ($0 < \lambda \leq 1$) according to eqn (1).

$$z_i = \lambda x_i + (1 - \lambda) z_{i-1} \quad (1)$$

Eqn (1). The equation for calculating exponentially weighted moving average values.

Author contributions

Conceptualization: MB, LW, IE, JE, PI, KH, HG. Methodology: LW, KJ, AH. Investigation: KJ, AH, PI, AF, VC, LB. Supervision: IE, MB, LW, LB, HG, KH. Writing—original draft: PI, JE, KJ, LW. Writing—review & editing: all authors.

Funding

Digital Cellulose Centre, a competence center set up by the Swedish Innovation Agency VINNOVA (grant no. 2016-05193) and a consortium of Swedish industries. 0-D-3D project financed by Swedish Foundation for Strategic Research (grant no. GMT14-0058).

Conflicts of interest

There are no conflicts to declare.

Acknowledgements

This work has been carried out in the Digital Cellulose Center, in which Agfa has kindly supplied PEDOT:PSS and Ahlstrom-Munksjö has kindly put their pilot paper machine to the project's disposal as well as offered analytical services (TGA, ionic demand and cross-section SEM/EDX). A special thanks to Robert Brooke at Research Institutes of Sweden who has created the conceptual visualization in Fig. 1B. We also acknowledge support from Treesearch, a collaboration platform for Swedish forest industrial research.

Notes and references

1 G. F. Frate, L. Ferrari and U. Desideri, *Renewable Energy*, 2021, **163**, 1754–1772.
2 O. Schmidt, S. Melchior, A. Hawkes and I. Staffel, Projecting the Future Levelized Cost of Electricity Storage Technologies, *Joule*, 2019, **3**, 81–100.
3 D. Larcher and J.-M. Tarascon, Towards greener and more sustainable batteries for electrical energy storage, *Nat. Chem.*, 2015, **7**, 19–29.
4 Z. Wang, Y. H. Lee, S. W. Kim, J. Y. Seo, S. Y. Lee and L. Nyholm, Why cellulose-based electrochemical energy storage devices?, *Adv. Mater.*, 2021, **33**, 2000892.
5 M. Baloch and J. Labidi, Lignin biopolymer: the material of choice for advanced lithium-based batteries, *RSC Adv.*, 2021, **38**, 23644.
6 Z. Wang, P. Tammela, M. Strømme and L. Nyholm, Cellulose-based Supercapacitors: Material and Performance Considerations, *Adv. Energy Mater.*, 2017, **7**, 1700130.
7 H. Zhu, W. Luo, P. N. Ciesielski, Z. Fang, J. Y. Zhu, G. Henriksson, M. E. Himmel and L. Hu, Wood-Derived Materials for Green Electronics, Biological Devices, and Energy Applications, *Chem. Rev.*, 2016, **116**, 9305–9374.
8 W. B. Hawley and J. Li, Electrode manufacturing for lithium-ion batteries—Analysis of current and next generation processing, *J. Energy Storage*, 2019, **25**, 100862.
9 O. Bubnova, A decade of R2R graphene manufacturing, *Nat. Nanotechnol.*, 2021, **16**, 1050.
10 M. G. Say, R. Brooke, J. Edberg, A. Grimoldi, D. Belaineh, I. Engquist and M. Berggren, Spray-coated paper supercapacitors, *npj Flex. Electron.*, 2020, **4**, 1–7.
11 P. Tammela, Z. Wang, S. Frykstrand, P. Zhang, I.-M. Sintorn, L. Nyholm and M. Strømme, Asymmetric supercapacitors based on carbon nanofibre and polypyrrole/nanocellulose composite electrodes, *RSC Adv.*, 2015, **5**, 16405–16413.
12 Y. J. Kang, S.-J. Chun, S.-S. Lee, B.-Y. Kim, J. H. Kim, H. Chung, S.-Y. Lee and W. Kim, All-Solid-State Flexible Supercapacitors Fabricated with Bacterial Nanocellulose Papers, Carbon Nanotubes, and Triblock-Copolymer Ion Gels, *ACS Nano*, 2012, **6**, 6400–6406.
13 X. Aeby, A. Poulin, G. Siqueira, M. K. Hausmann and G. Nyström, Fully 3D Printed and Disposable Paper Supercapacitors, *Adv. Mater.*, 2021, **33**, 2101328.
14 B. Andres, C. Dahlström, N. Blomquist, M. Norgren and H. Olin, Cellulose binders for electric double-layer capacitor electrodes: The influence of cellulose quality on electrical properties, *Mater. Des.*, 2018, **141**, 342–349.
15 L. Jabbour, D. Chaussy, B. Eyraud and D. Beneventi, Highly conductive graphite/carbon fibre/cellulose composite papers, *Compos. Sci. Technol.*, 2012, **72**, 616–623.
16 Y.-R. Kang, Y.-L. Li, F. Hou, Y.-Y. Wen and D. Su, Fabrication of electric papers of graphenenanosheet shelled cellulose fibres by dispersion and infiltration as flexible electrodes for energy storage, *Nanoscale*, 2012, **4**, 3248–3253.
17 R. Brooke, J. Edberg, M. G. Say, A. Sawatdee, A. Grimoldi, J. Åhlin, G. Gustafsson, M. Berggren and I. Engquist, Supercapacitors on demand: all-printed energy storage devices with adaptable design, *Flex. Print. Electron.*, 2019, **4**, 015006.
18 D. Klemm, F. Kramer, S. Moriz, T. Lindström, M. Ankerfors, D. Gray and A. Dorris, Nanocelluloses: A New Family of Nature-Based Materials, *Angew. Chem., Int. Ed.*, 2011, **50**, 5438–5466.
19 Y. Peng, D. J. Gardner and Y. Han, Drying cellulose nanofibrils: in search of a suitable method, *Cellulose*, 2012, **19**, 91–102.
20 P. Tammela, S. Yamada and L. Sandberg, *Method of Preparing Cellulose Fibres Coated with Redox-Active Polymer*, World Intellectual Property Organization, 2020, WO 2020/260323 A1.
21 K. V. G. Raghavendra, R. Vinoth, K. Zeb, C. V. V. M. Gopi, S. Sambasivam, M. R. Kummara, I. M. Obaidat and H. J. Kim, An intuitive review of supercapacitors with recent progress and novel device applications, *J. Energy Storage*, 2020, **31**, 101652.
22 D. Belaineh, R. Brooke, N. Sani, M. G. Say, K. Håkansson, I. Engquist, M. Berggren and J. Edberg, Printable carbon-based supercapacitors reinforced with cellulose and conductive polymers, *J. Energy Storage*, 2022, **50**, 104224.
23 G. A. Tafete, M. K. Abera and G. Thothadri, Review on nanocellulose-based materials for supercapacitors applications, *J. Energy Storage*, 2022, **48**, 103938.
24 K. Jain, M. S. Reid, P. A. Larsson and L. Wågberg, On the interaction between PEDOT:PSS and cellulose: Adsorption mechanisms and controlling factors, *Carbohyd. Polym.*, 2021, **260**, 117818.
25 R. Brooke, A. Fall, M. Borràs, D. Belaineh, J. Edberg, S. Martinez-Crespiera, C. Aulin and V. Beni, Nanocellulose based carbon ink and its application in electrochromic displays and supercapacitors, *Flex. Print. Electron.*, 2021, **6**, 045011.
26 H. Sehaqui, U. Perez de Larraya, P. Tingaut and T. Zimmermann, Humic acid adsorption onto cationic cellulose nanofibers for bioinspired removal of copper(ii) and a positively charged dye, *Soft Mat.*, 2015, **11**, 5294–5300.
27 A. Pei, N. Butchosa, L. A. Berglund and Q. Zhou, Surface quaternized cellulose nanofibrils with high water absorbency and adsorption capacity for anionic dyes, *Soft Mat.*, 2013, **9**, 2047–2055.
28 S. Soares, G. Camino and S. Levchik, Comparative study of the thermal decomposition of pure cellulose and pulp paper, *Polym. Degrad. Stab.*, 1995, **49**, 275–283.
29 J. Y. Hwang, M. Li, M. F. El-Kady and R. B Kaner, Next-Generation Activated Carbon Supercapacitors: A Simple Step in Electrode Processing Leads to Remarkable Gains in Energy Density, *Adv. Funct. Mater.*, 2015, **27**, 1605745.
30 A. Svedberg and T. Lindström, The effect of various retention aids on retention and formation, *Nord. Pulp Pap. Res. J.*, 2010, **25**, 195–203.
31 D. Solberg and L. Wågberg, On the mechanism of GCC filler retention during dewatering – New techniques and initial findings, *J. Pulp Pap. Sci.*, 2002, **28**, 183–188.

32 W. W. Sampson and P. J. Turner, The effect of suspension crowding on the in-plane distribution of filler in handsheets, *Appita J.*, 1996, **49**, 274–276.
33 T. Lindström, L. Wågberg and T. Larsson, Paper presented at the 13th fundamental research symposium, 2005, Cambridge, UK.
34 S. H. Osong, S. Norgren and P. Engstrand, Paper strength improvement by inclusion of nano-lignocellulose to Chemi-thermomechanical pulp. Nord, *Pulp Pap. Res. J.*, 2014, **29**, 309–316.
35 A. Tanaka, K. Niskanen, E. Hiltunen and H. Kettunen, Inter-fibre bonding effects of beating, starch or filler, *Nord. Pulp Pap. Res. J.*, 2001, **16**, 306–312.
36 R. Brooke, J. Åhlin, K. Hübscher, O. Hagel, J. Strandberg, A. Sawatdee and J. Edberg, Large-scale paper supercapacitors on demand, *J Energy Storage*, 2022, **50**, 104191.
37 B.-H. Xiao, R.-T. Lin, K. Xiao and Z.-Q. Liu, A highly compressible, nitrogen doped carbon foam based all pseudo-capacitance asymmetric supercapacitors, *J. Power Sources*, 2022, **530**, 231307.
38 S. Kormakov, D. Wu, J. Sun, X. Gao, X. He, X. Zheng and Z. Zhi, The electrical conductive behaviours of polymer-based three-phase composites prepared by spatial confining forced network assembly, *EXPRESS Polym. Lett.*, 2019, **13**, 713–723.
39 T. Guo, M. Fu, D. Zhou, L. Pang, J. Su, H. Lin, X. Yao and A. S. B. Sombra, Flexible Ti3C2Tx/Graphene Films with Large-Sized Flakes for Supercapacitors, *Small Struct.*, 2021, **2**, 2100015.
40 X.-X. Li, X.-H. Deng, Q.-J. Li, S. Huang, K. Xiao, Z.-Q. Liu and Y. Tong, Hierarchical double-shelled poly(3,4-ethylenedioxythio-phene) and MnO_2 decorated Ni nanotube arrays for durable and enhanced energy storage in supercapacitors, *Electrochim. Acta*, 2018, **264**, 46–52.
41 G.-F. Chen, X.-X. Li, L.-Y. Zhang, N. Li, T. Y. Ma and Z.-Q. Liu, A Porous Perchlorate-Doped Polypyrrole Nanocoating on Nickel Nanotube Arrays for Stable Wide-Potential-Window Supercapacitors, *Adv. Mater.*, 2016, **28**, 7680–7687.
42 S. Cao, H. Zhang, Y. Zhao and Y. Zhao, Pillararene/Calixarene-based systems for battery and supercapacitor applications, *eScience*, 2021, **1**, 28–43.
43 Y.-R. Tsai, B. Vedhanarayanan, T.-Y. Chen, Y.-C. Lin, J.-Y. Lin, X. Ji and T.-W. Lin, A tailor-made deep eutectic solvent for 2.2 V wide temperature-tolerant supercapacitors *via* optimization of *N*,*N*-dimethylformamide/water co-solvents, *J. Power Sources*, 2022, **521**, 230954.
44 V. V. Obreja, A. Dinescu and A. C. Obreja, Activated carbon based electrodes in commercial supercapacitors and their performance, *Int. Rev. Electr. Eng.*, 2010, **5**, 272–281.
45 V. V. N. Obreja, *Paper Presented at the 1st International Freiberg Conference on Electrochemical Storage Materials*, Freiberg, DE, June 03-04 2013.
46 Z. Li, Z. Xu, X. Tan, H. Wang, C. M. Holt, T. Stephenson, B. C. Olsen and D. Mitlin, Mesoporous nitrogen-rich carbons derived from protein for ultra-high capacity battery anodes and supercapacitors, *Energy Environ. Sci.*, 2013, **6**, 871–878.
47 D. Wang, Z. Geng, B. Li and C. Zhang, High performance electrode materials for electric double-layer capacitors based on biomass-derived activated carbons, *Electrochim. Acta*, 2015, **173**, 377–384.
48 A. Pei, N. Butchosa, L. A. Berglund and Q. Zhou, Surface quaternized cellulose nanofibrils with high water absorbency and adsorption capacity for anionic dyes, *Soft Matter*, 2013, **9**, 2047–2055.
49 L. Wågberg, L. Winter, L. Ödberg and T. Lindström, On the charge stoichiometry upon adsorption of a cationic polyelectrolyte on cellulosic materials, *Colloid. Surface.*, 1987, **27**, 163–173.
50 P. Isacsson, X. Wang, A. Fall, D. Mengistie, E. Calvié, H. Granberg, G. Gustafsson, M. Berggren and I. Engquist, Highly Conducting Nanographite-Filled Paper Fabricated *via* Standard Papermaking Techniques, *ACS Appl. Mater. Inter.*, 2020, **12**, 48828–48835.
51 P.-Å. Johansson and B. Norman, *Paper Presented at the Process and Product Quality Conference*, Cincinnati, OH, USA, October 14-17 1996.
52 S. W. Roberts, Control Chart Tests Based on Geometric Moving Averages, *Technometrics*, 1959, **1**, 239–250.
53 H. K. Song, H.-Y. Hwang, K.-H. Lee and L. H. Dao, The effect of pore size distribution on the frequency dispersion of porous electrodes, *Electrochim. Acta*, 2000, **45**(14), 2241–2257.
54 H. D. Yoo, J. H. Jang, J. H. Ryu, Y. Park and S. M. Oh, Impedance analysis of porous carbon electrodes to predict rate capability of electric double-layer capacitors, *J. Power Sources*, 2014, **267**, 411–420.